Journal of Materials Chemistry C

Accepted Manuscript

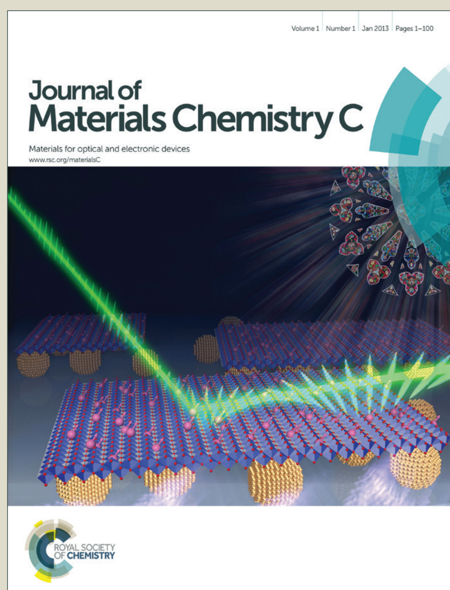

This is an *Accepted Manuscript*, which has been through the Royal Society of Chemistry peer review process and has been accepted for publication.

Accepted Manuscripts are published online shortly after acceptance, before technical editing, formatting and proof reading. Using this free service, authors can make their results available to the community, in citable form, before we publish the edited article. We will replace this *Accepted Manuscript* with the edited and formatted *Advance Article* as soon as it is available.

You can find more information about *Accepted Manuscripts* in the Information for Authors.

Please note that technical editing may introduce minor changes to the text and/or graphics, which may alter content. The journal's standard Terms & Conditions and the Ethical guidelines still apply. In no event shall the Royal Society of Chemistry be held responsible for any errors or omissions in this *Accepted Manuscript* or any consequences arising from the use of any information it contains.

ROYAL SOCIETY OF CHEMISTRY

www.rsc.org/materialsC

Journal Name

RSCPublishing

ARTICLE

Cite this: DOI: 10.1039/x0xx00000x

Received 00th January 2012,
Accepted 00th January 2012

DOI: 10.1039/x0xx00000x

www.rsc.org/

Ultrahigh Photo-responsivity and Detectivity in Multilayer InSe nanosheets Phototransistors with Broadband Response from Ultraviolet-Visible to Near Infrared Light

Wei Feng,[a, e] Jing-Bin Wu,[b] Xiaoli Li,[b] Wei Zheng,[a] Xin Zhou,[f] Kai Xiao,[d] Wenwu Cao,[c] Bin Yang,[c] Weiquan Tian,[f] PingHeng Tan,[b*] PingAn Hu[a*]

We demonstrate the strategies and principles for the performance improvement of layered semiconductor based photodetectors using multilayer indium selenide (InSe) as the model materials. It is discovered that multiple reflection interference at the interfaces in phototransistor device leads to thickness-dependent photo-response, which provide a guideline to improve the performance of layered semiconductor based phototransistors. The responsivity and detectivity of InSe nanosheets phototransistor can be adjustable using applied gate voltage. Our InSe nanosheets phototransistor exhibits ultrahigh responsivity and detectivity. An ultrahigh external photo-responsivity of ~10^4 AW^{-1} can be achieved during broad spectra ranging from UV to near infrared wavelength from our InSe nanosheets photodetectors. The detectivity of multilayer InSe devices is ~ 10^{12} ~ 10^{13}Jones, which surpasses that of currently-exploited InGaAs photodetectors (10^{11} ~ 10^{12} Jones). This research shows that multilayer InSe nanosheets are promising materials for high performance photodetectors.

Introduction

Broadband sensing from ultraviolet (UV)-visible to the near infrared (NIR) wavelength has various applications in image sensing, communications, environmental monitoring, and remote control.[1-5] Traditionally, separate sensors or materials are used for different sub-bands in the range from UV to NIR wavelength.[1-3] For example, gallium nitride (GaN), silicon (Si) and Indium-Gallium-Arsenide (InGaAs) are commonly used for sensing of UV, visible and NIR lights, respectively. [4, 5] The photo-responsivity for GaN and –Si based photodetectors is below 0.2 AW^{-1}, and the responsivity for InGaAs device is usually less than 1 AW^{-1}.[4, 5] The detectivity for silicon photodetectors is ~ 4×10^{12} Jones (1 Jones = 1 cm $H_Z^{1/2}$/W), and a typical detectivity of InGaAs is greater than 10^{12} Jones when it is cooled down to 4.2 K. [4, 5] It would be greatly advantageous to have a broadband photodetectors system with high sensitivity, fast speed, wide spectral response from UV to NIR, and high detectivities achievable at room temperature.

A small band-gap semiconducting polymer blended with a fullerene derivative was used to fabricate high detectivity photodetectors with a wide spectral response from UV to NIR. This polymer photodetector exhibited a high detectivity greater than 10^{12} Jones at room temperature, but a low photo-responsivity of only 0.17 AW^{-1}.[6] PbS colloidal quantum dots were exploited to give broadband response ranging from UV to NIR, exhibiting an ultrahigh responsivity of > 10^3 AW^{-1} and a high detectivity of 1.8×10^{13} Jones at wavelength of 1.3 μm at room temperature.[7] However, the lateral structure adopted in these PbS quantum dot photodetectors leads to a large driving voltage of ~ 100 V and a slow response, which limit their practical applications.

Recently, two-dimensional (2D) layered semiconductors such as transition-metal chalogenides (e.g. MoS_2, WS_2, GaS, GaSe) have been demonstrated attractive capabilities for optoelectronics due to ultrathin thickness, atomic flatness and the facile manipulation as well as their tunable optical properties controlled by thickness.[8-15] These 2D ultrathin materials are usually obtained by "Scotch-tape" mechanical exfoliation, in view of layered structures with the weak van der Waals interaction between adjacent layers. Compared to traditional semiconducting films such as silicon or Ш-V

Journal of Materials Chemistry C Accepted Manuscript

semiconductors, 2D layered materials have more ideal surfaces free of dangling bonds, which reduces surface roughness scattering (leading to high mobilities) and interface traps (resulting in low density of interface state on the semiconductor-dielectric interface); Atomic thickness of 2D layered films allows more efficient electrostatics by gate voltage; And 2D layered films exhibit intriguing physical behaviour strongly dependent on the layer number (thickness), such as the band-gap structure transition of MoS_2 from an indirect structure in the bulk to a direct one in monolayer. These unique features make 2D semiconductor nanosheets a new class of materials with superior properties, which are key to the applications in electronics and optoelectronics. Recently, new optoelectronic devices have been demonstrated using various 2D nanosheets.[8, 14-20] Single-layer or multilayer MoS_2-based photodetectors have tunable spectral photoresponse [10,17] and are ultrasensitive to visible light, with photoresponsivities reaching as high as 880 AW^{-1}.[17] However, ultralow response time (~4 s) hinders its practical application. UV-visible photodetectors based on few-layer GaSe and GaS nanosheets exhibit responsivities of 2.8 AW^{-1} and 19.2 AW^{-1}, respectively.[14, 15] A low photoresponse of 34.7 mAW^{-1} was measured in few-layer InSe.[16] And UV - near IR photodetectors based on multilayer InSe[18] and In_2Se_3[19] show high responsivities of 12.3 AW^{-1} and 395 AW^{-1}, respectively. Also, multilayer GaTe photodetectors have been demonstrated to have a very high photoresponsivity of 10^4 AW^{-1} for UV-visible light.[20] It is still challenging to make phototransistors with both ultrahigh photo-responsivity and detectivity, and having broadband spectra response. Especially, there is few reports about thickness dependent photo-response in 2D layered semiconductors, which is a key issue in the devices constructed using the ultrathin layered materials.

Here, we demonstrate broadband, ultrahigh responsivity multilayer InSe nanosheets phototransistors, which have a wide spectral response ranging from UV to NIR lights. Our results confirm that multiple reflection interference at the interfaces in the Air/InSe/SiO_2/Si multilayer configuration leads to the thickness-dependent photo-response, which provides a useful guideline to improve the performance of layered semiconductor phototransistors. The performance (responsivity, detectivity) of multilayer InSe nanosheets phototransistors can be efficiently tuned by applying gate voltage. A maximum external photoresponsivity of 5.6×10^4 AW^{-1} at the UV wavelength of 254 nm, 3×10^4 AW^{-1} at the visible light of 700 nm and 2×10^3 AW^{-1} at the NIR light of 850 nm have been achieved from InSe nanosheets phototransistors. At room temperature, the detectivity of InSe nanosheets phototransistors are 2×10^{13} Jones at the UV-visible band, and 10^{12} Jones at the NIR band, which greatly surpass those of silicon photodetectors. Furthermore, these InSe devices exhibit a fast response time of ~5 ms. The superior performances in InSe nanosheets photodetectors are mainly owing to high surface ratio, high carrier mobility combined with narrow gap and direct band structures.

Experimental

Synthesis and characterization of InSe nanosheets: The bulk InSe crystal was prepared by using the modified Bridgman method. The multilayer InSe nanosheets were mechanically exfoliated from bulk InSe crystals and transferred onto the silicon substrate coated with 285 nm SiO_2. The thickness was determined by using atomic force microscopy (AFM, Nanoscope IIIa Vecco). The structure and composition of multilayer InSe nanosheets were identified by X-ray diffraction (XRD, DIFFRACTOMETER-6000 with Cu Ka radiation (λ= 0.1542 nm)) and transmission electron microscopy (Tacnai-G2 F30, accelerating voltage of 300 kV) attached with an energy-dispersion X-ray spectroscopy (EDS).

Fabrication of InSe FETs and photodetectors: The multilayer InSe nanosheets were transferred to the SiO_2/Si substrates. Cr/Au electrodes with 5 nm thick Cr and 35 nm thick Au were fabricated using a shadow mask. The transistors based Si/SiO_2 substrates were annealed at 200 ℃ for 30 min with 100 sccm Ar : H_2 (V/V = 9/1) to reduce the resistance and improve the contact for the devices.

Characterizations of electronic and optoelectronic properties: Electrical characterizations of transistors based on InSe nanosheets devices were performed by using semiconductor characterization system (Keithley 4200 SCS) with a Lakeshore probe station. Mono-chromatic lights of 254-850 nm were obtained by using optical filters using a 500 W xenon lamp as the light source. The photocurrent measurements were performed by semiconductor characterization system (Keithley 4200 SCS) with a Lakeshore probe station. The intensities of incident light source were identified by a power and energy meter (Model 372, Scienteck).

Results and discussion

InSe is a highly promising material for applications in optoelectronics, radiation detectors and solar energy conversion devices due to its small direct band-gap of 1.26 eV at room temperature.[21-25] InSe crystals in this study were synthesized by

Journal of Materials Chemistry C Accepted Manuscript

This journal is © The Royal Society of Chemistry 2012

using elemental indium and selenide as precursors (detailed in the experimental section). The crystalline structure of the as-prepared crystal is the β-type determined by X-ray diffraction (XRD) (Fig. S1, supporting information) measurement. The *β*-InSe is composed of vertically stacked Se-In-In-Se sheets with weak bonding between adjacent sheets via the van der Waals force. Figure 1a shows crystal structure of *β*-InSe sheet with a thickness of 6.2 Å and a top view of InSe single sheet crystal structure with typical hexagonal. Figure 1b presents a low magnification TEM image of InSe nanosheets with an inset for the selected area electron diffraction pattern (SEAD) provides another evidence for the formation of single crystalline *β*-InSe flakes with an orientation along [100] zone axis. Figure 1c shows an atomic-resolution scanning transmission electron microscopy (AR-STEM) image, which shows an ideal hexagonal lattice structure, with a lattice spacing of 0.34 nm, corresponding to the lattice constant of (100) direction. In/Se atomic ratio was calculated to be 1:1 by the energy-dispersive X-ray spectroscopy (EDS) (Fig. S2, supporting information). Multilayer InSe nanosheets can be exfoliated from a bulk crystal and transferred to SiO_2/Si substrates.

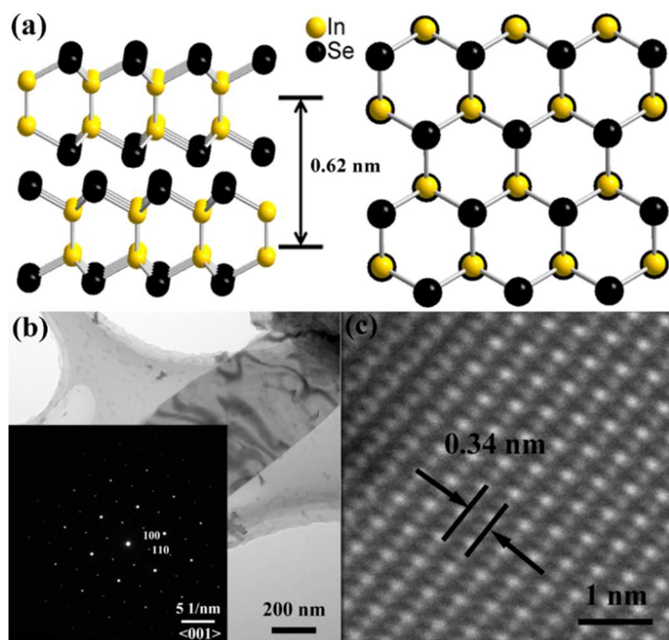

Fig. 1 Crystal structure and characterization of InSe nanosheets. (a) Crystal structure of InSe, The left part is the side view, and the right part is the top view; (b) TEM images of multilayer InSe at low magnification; Inset: The corresponding SAED pattern; (c) z-contrast STEM image showing the atomic structure of InSe nanosheets.

Photon absorption is a very important physical process that determines the performance of layered materials based photodetectors. We performed the theoretical simulations of light absorption inside InSe nanosheets lying on SiO_2/Si substrates as a function of the thickness, where SiO_2 thickness is 285 nm. The absorption is determined by multiple reflection interference at the interfaces and in the interlayers and the complex refractive indices of each medium in the multilayer configuration. The multilayer optical interference method[26, 27] has been widely used to quantify the optical contrast[27, 28] and the Raman intensities[26, 29-32] of ultrathin flakes of 2D crystals. Here, we adopt this method to study photon absorption of InSe nanosheets deposited on the SiO_2/Si substrate when the light is vertically incident onto the InSe nanosheets.

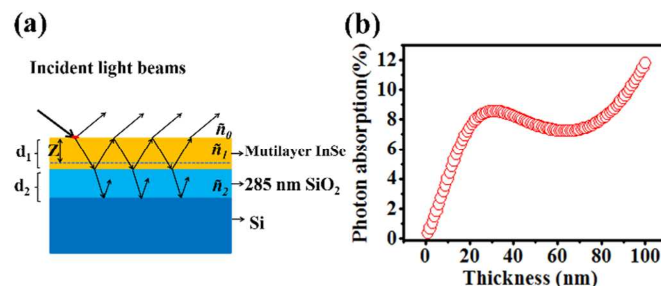

Fig. 2 (a) Schematic for the photon absorption of InSe multilayer on the SiO2/Si substrate; (b) Thickness-dependent photo absorption.

A multilayer configuration, Air/InSe/SiO_2/Si, is proposed as shown in Fig. 2a, where air, InSe, SiO_2 and Si layers are, respectively, denoted by indices i = 0, 1, 2, and 3. The corresponding thickness and complex refractive indices are designated by d_i and $\check{n}_i(\lambda) = n_i(\lambda) - ik_i(\lambda)$, where the n_i and k_i values are functions of wavelength (λ) for InSe[33], SiO_2[34] and Si[34]. The total photon absorption in the whole InSe layer can be expressed as:

$$\gamma_{ab} \propto \int_0^{d_1} \beta(|F_{ab}(Z)|^2)dZ$$

Where $\beta = 4\pi k_1/\lambda$ is absorption coefficient of the bulk InSe, F_{ab} is the enhancement factor from multilayer optical interference effect, following the notation by Duhee Yoon[26] and Naeyoung Jung[30]. In the calculations, the electric field amplitude of the incident photons has been normalized, so $F_{ab}(Z)$ denotes the electric field amplitude of the incident photons at depth Z in the InSe layer[29, 32]. For convenience, we calculated $F_{ab}(Z)$ by means of the transfer matrix method. [27, 28, 31] Then, we can get the total photon absorption in the whole InSe layer with a thickness of d_1 by integrating over the InSe thickness, as represented by the above equation. As an example, Fig. 2b shows the total photon absorption of the InSe flakes dependent on the thickness in a range of 1 nm-100 nm when the photon wavelength is set to 700 nm. The total photon absorption exhibits a peak around the thickness of 30 nm, which means that there exists an optimized thickness of the InSe layer for application in photon

Journal of Materials Chemistry C Accepted Manuscript

detectors. The theoretical simulations of light absorption of InSe nanosheets deposited on SiO_2/Si substrate suggests that 30-40 nm InSe nanosheets are optimal channel for high performance photodetectors because of the direct band-gap and best phonon absorption.

The InSe field effect transistors (FETs) and phototransistors are fabricated using Cr/Au contacts on 285 nm SiO_2/Si substrates. Fig. 3a describes the schematic structure of the device in this study. Electrical properties and optoelectronic characterizations are measured with back gate structure at room temperature in ambient condition. The thickness of InSe nanosheets is in the range of 4~60 nm, which is measured by atomic force microscopy (AFM).

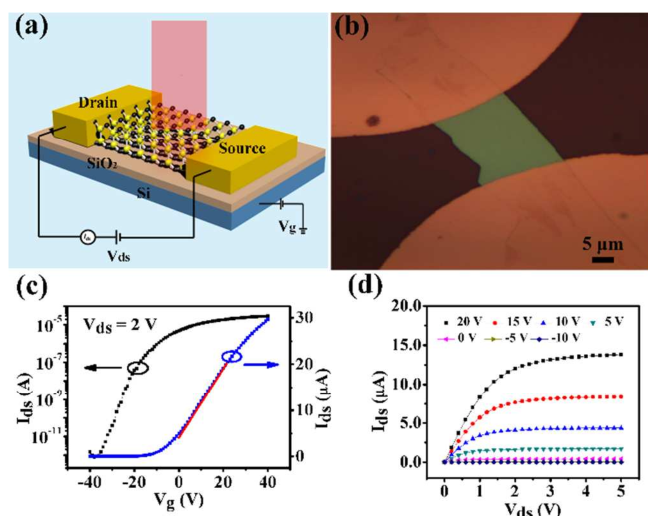

Fig. 3 Multilayer InSe nanosheets transistor and phototransistor. (a) Schematic drawing of a phototransistors based on InSe nanosheets; (b) A typical image of the InSe nanosheets; (c) A typical transfer curve of InSe nanosheets transistor; (d) Corresponding output curve of InSe nanosheets transistors.

The fabricated multilayer InSe FETs (Fig. 3b, channel length ~20 μm, width ~15 μm, and Fig. S3: thickness of channel ~30 nm) shows a typical n-type FET properties (Fig. 3c-3d). The I_{ds}-V_{ds} characteristics agree with the conventional long-channel n-type MOS transistor, showing a linear regime under low V_{ds} and a saturation regime under high V_{ds}. This feature is an important factor for practical applications since thin film transistors (TFTs) in organic light emitting diode (OLED) displays are working at the saturation current region. InSe FETs show the saturation of drain current because the conducting channel is converted to "pinch-off" condition at high V_{ds}. The current on/off ratio is calculated by adopting ratio of maximum to minimum I_{ds} from the plot of V_g *vs* I_{ds}. The current on/off ratio is 10^7 for this device. The mobility of multilayer InSe transistors can be extracted using the equation $\mu = [L/(W\times(\varepsilon_0\varepsilon_r/d)\times V_{ds})]\times dI_{ds}/dV_g$, where L = 20 μm is length of transistor, W = 15 μm is width of transistor, $\varepsilon_0 = 8.854 \times 10^{-12}$ Fm^{-1} is the vacuum permittivity, ε_r is 3.9 for SiO_2 and d (285 nm) is the thickness of SiO_2. The mobility of the transistor is calculated to be 32.6 $cm^2V^{-1}s^{-1}$ in ambient environment (Fig. 3c, V_{ds}= 2 V). High carrier mobility can promote the photocurrent inside multilayer InSe nanosheets device.

To measure the photoresponse of multilayer InSe nanosheets devices on SiO_2/Si substrates, monochromatic light illumination was directed vertically onto devices consisting of two Cr/Au electrodes and InSe nanosheets channel with a 20 μm length and a 15 μm width (depicted in Fig. 3). Optoelectronic characterizations were recorded with a fixed illumination intensity of 0.29 $mWcm^{-2}$ under the different illumination wavelengths ranging from 254 nm to 850 nm (Fig. 4a and 4b). The device shows a broad spectral response to light from the ultraviolet to the near infrared regions. The I_{ds}-V_{ds} curves shown in Fig. 4a exhibit a significant increase of source-drain current by one order of magnitude as the device is illuminated. Accordingly, the photocurrents I_{ph} ($I_{ph} = I_{illumination} - I_{dark}$) also increase with the bias voltage V_{ds}, which is due to the increase in carrier drift velocity and the related decrease of carrier transit time T_t.

The dependence of photocurrent on the gate bias was investigated under illumination of 254 nm, 490 nm, 700 nm and 850 nm light with a fixed illumination intensity of 0.29 $mWcm^{-2}$ and bias voltage of 5 V (shown in Fig. 4b). The ratio of photocurrents at ON state versus OFF state can reach an order of 10^6, so that the photocurrent flowing through whole circuit is efficiently controlled by applying gate voltage. In both OFF and ON states the device current increases across the whole gate voltage range employed. This indicates that the photocurrent dominates over thermionic and tunnelling currents across the entire operating range of gate voltages.

The observed gate dependent behaviour of multilayer InSe nanosheets phototransistors can be explained by a simple energy band diagram (Fig. 4c). When metal electrodes are contacted with InSe nanosheets, a charge transfer occurs at the interfaces via Femi level tuning at an equilibrium, which causes the accumulation of space charges in the contact region together with a band bending to form Schottky type barriers as well as a depletion layer. As the OFF state devices are illuminated ($V_g < V_t$), light absorption and excitations of hole-electron pairs occur, which can be extracted to generate photocurrent by applying a bias. The photocurrent increases with decreasing wavelength because the higher excitation energy

Journal of Materials Chemistry C Accepted Manuscript

 This journal is © The Royal Society of Chemistry 2012

provided by higher photon energies can produce more excitations. In the ON state ($V_g > V_t$), photo-excited current and the thermionic, tunnelling currents all contribute to the device current. Increasing gate voltage can shift down the band and decrease the depletion layer to lower the barrier heights at contacts, resulting in more efficient photocurrent extraction and enhanced photoresponse.

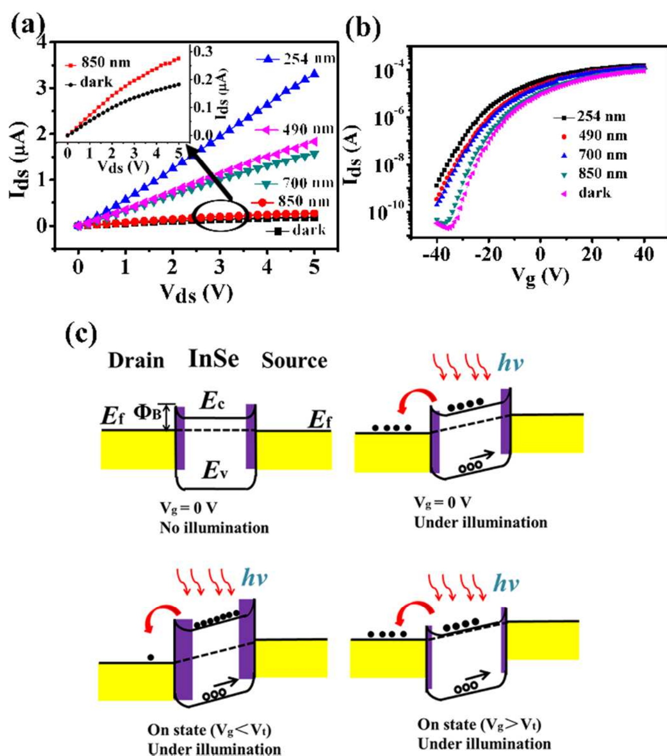

Fig. 4 Photoinduced response of multilayer InSe nanosheets phototransistor. (a) Drain-source (I_{ds}-V_{ds}) characteristic of the device at V_g = 0 V and under the different illumination wavelength with light intensity of 0.29 mW/cm^2; Inset is enlarged phototcurrrent under 850 nm illumination. (b) Gating response (I_{ds}-V_g) of the InSe phototransistor in the dark and under the illumiations of 254 nm, 490 nm,700 nm and 850 nm lights with intensity of 0.29 mW/cm^2 at V_{ds} = 5 V. (c) Band digaram of InSe nanosheet phototransistor: E_F is the Fermi level energy, E_c the minimum conduction band energy, E_v maximum valence band energy and Φ_B barrier height.

Responsivity (R_λ) is a critical parameter to evaluate the performance of a phototransistor. The R_λ is defined as the photocurrent generated per unit power of the incident light on the effective area of a phototransistor[20] The R_λ value can be calculated as the following equations: $R_\lambda = I_\lambda / P_\lambda S$. Here, I_λ is the generated photocurrent, P_λ is the incident light intensity, S (300 μm^2) is the effective illuminated area. Fig. 5a shows gate dependent responsivity (R_λ) acquired at bias voltage V_{ds} = 5 V. Responsivity is also highly tunable by the applied gate voltage (shown in Fig. 5a). For example, responsivity measured under the illumination of 254 nm ($R_{245\ nm}$) increases from 1.65×10^{-3} AW^{-1} at V_g = -40 V (OFF state) to 2.31×10^4 AW^{-1} at V_g = 0, and to 5.68×10^4 AW^{-1} at V_g = 40 V (ON state). Our InSe nanosheets phototransistors are super-responsive to a broad spectral range from UV-visible to NIR, as shown in Fig. 5b. Responsivity measured under broadband illumination of ultraviolet (254 nm), visible (490 nm, 700 nm) and near infrared light (850 nm) are $R_{254\ nm}$= 5.68×10^4 AW^{-1}, $R_{490\ nm}$ = 3.574×10^4 AW^{-1}, $R_{700\ nm}$ = 3.06×10^4 AW^{-1} and $R_{850\ nm}$ = 2.975×10^3 AW^{-1}, respectively. The responsivities of our multilayer InSe nanosheets photodetectors are much higher than those of currently used silicon or InGaAs photodetector (< 2 AW^{-1}), even largely surpass all presently reported values for other 2D layered materials based optoelectronics[8, 14-20] (see more information in Table S1).

Another important parameter to evaluate the performance of photodetectors is the specific detectivity (D*). The normalized detectivity D* is measured in units of Jones (cm $Hz^{1/2}W^{-1}$). D* is given as $(A\triangle f)^{1/2}R/in$, where A is the effective area of the detector in cm^2, $\triangle f$ is the electrical bandwidth in Hz, and R is the responsivity in AW^{-1} measured under the same conditions as the noise current (in Amperes). The material figure of merit D* allows comparison among devices of different areas and geometries. There are three contributions to the total noise that limit D*: shot noise from dark current, Johnson noise, and thermal fluctuation noise. The shot noise from the dark current is the major contributor to the total noise in this case, the detectivity can be calculated by the equation: $D^* = RA^{1/2}/(2eI_d)^{1/2}$, where R is responsivity, A is the area of the phototransistor channel, e is the electron charge, and I_d is the dark current.[3] Fig. 5b shows the calculated D* of a phototransistor at different wavelengths. the D* is ~10^{13} Jones for visible light and ultraviolet region and ~10^{12} Jones for NIR, which both surpass the D* values of currently used Si or InGaAs photodetectors (~10^{11}-10^{12} Jones)[4, 5], and MoS_2, In_2Se_3 devices (~10^{11} -10^{12} Jones).[17, 19]

The theoretical simulations of light absorption of InSe nanosheets deposited on SiO_2/Si substrate indicates that the thickness is crucial element for achieving high performance of photodetectors. The Fig. 5c shows the responsivity as a function of thickness, which were measured with 700 nm light illumination at a light intensity of 0.29 mW cm^{-2} under a bias of 5 V. Photoresponse increases from 10 nm to 40 nm and then starts to decrease with thickness. The responsivity is proportion to photocurrent, and photocurrent is mainly dependent on light absorption. Theoretical simulation shows that there is a peak between 30-40 nm for light absorption of InSe nanosheets. Experiment results can be explained by former simulation. Maximum photoresponse is achieved at a

Journal of Materials Chemistry C Accepted Manuscript

thickness of about 40 nm, whereas maximum photon-adsorption was obtained at ~30 nm (shown in Fig. 2c). Photocurrent generation consists of photon-adsorption, photo-carrier generation and the photocurrent generation through extraction and transport. Actually, a 30-nm thick InSe sheet shows an adsorption of 8.96%, which is a little different from that of 40 nm InSe with an adsorption of 7.91%. Under almost same photo-adsorption rate, other factors (photo-carrier generation or photo-carrier transport) influenced by the thickness will further modify the optimized thickness, which need to be further investigated.

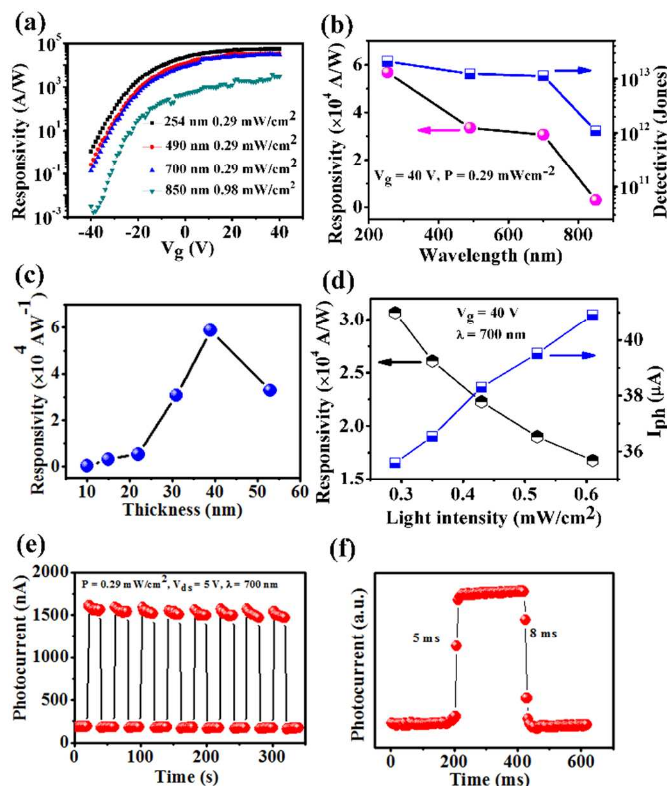

Fig. 5 Photoresponse performance of multilayer InSe phototransistor. (a) Gate voltage dependent responsivity under a bias voltage V_{ds} = 2 V and light intensity P = 0.29 mW cm^{-1} under the illumination of lights with wavelengths of 254 nm, 490 nm, 700 nm and 850 nm; (b) Responsivity and detectivity as a function of illumination wavelengths with light intensity P = 0.29 mW cm^{-1} at the gate bias V_g = 40 V; (c) Responsivity as function of InSe thickness; (d) Responsivity and photocurrent as a function of illumination intensity under wavelength of 700 nm at the gate bias V_g = 40 V (e),(f)Time-resolved photoresponse of InSe photodetector under the illumination of 700 nm light with the voltage V_{ds} = 5 V and light intensity P = 0.29 mW cm^{-1}.

When the photon energy is higher than the E_g of InSe, the generated photocurrent is controlled by the illuminated intensity. Fig. 5d shows I_{ph} as a function of illumination intensity under 700 nm at the gate bias V_g = 40 V. The generated I_{ph} increase gradually with the light intensity increasing from 0.29 $mWcm^{-2}$ to 0.61 $mWcm^{-2}$. In other words, multilayer InSe phototransistors can generate a light intensity dependent I_{ph}. The good linear between I_{ph} and light intensity confirms that generated photocurrent is determined by the quantity of photogenerated carriers under illumination. As the illumination intensity is increased, the responsivity is degraded, which is due to the trap states existed InSe or at the interface between InSe and the dielectric substrate.

The response speed is another important parameter of photodetectors. The temporal response of our multilayer InSe nanosheets phototransistors was characterized using a chopper generated short light pulse. Figure 5e, 5f show the transient photocurrent of our InSe nanosheets device measured under a bias of 5 V at a light intensity of 0.29 mW cm^{-2}. With the light irradiation at 700 nm on and off, our InSe nanosheets photodetectors exhibit repeatable and stable response to incident light. Response time is calculated by averaging the duration values between light-ON and light-OFF (Corresponding to 80% increase or decay). The measured rise and fall time are 5 ms and 8 ms, respectively, which are much faster than that of single-layer MoS_2 devices (response time: 50 ms).[8]

Conclusions

In summary, we have demonstrated multilayer InSe nanosheets transistors and phototransistors. The photon adsorption inside InSe nanosheets exhibits a strong dependence on the thickness, which is originated from multiple reflection interference at the interfaces of the Air/InSe/SiO_2/Si multilayer configuration. The multilayer InSe transistors show an intrinsic n-type semiconductor conductance and exhibit a high mobility of 32 $cm^2V^{-1}s^{-1}$ and a high current on/off ratio ~10^7. The multilayer InSe nanosheets phototransistors have a broad spectral response from UV to NIR light. The performance (photoresponsivity, detectivity) of multilayer InSe nanosheets phototransistors can be efficiently controlled by the applied gate voltage. Maximum external photoresponsivities of 5.6×10^4 AW^{-1} at the UV wavelength of 254 nm, 3×10^4 AW^{-1} at the visible light of 700 nm and 2×10^3 AW^{-1} at the NIR light of 850 nm have been achieved. At room temperature, the detectivities of InSe nanosheet photodetectors are 2×10^{13} Jones at UV-visible wavelength, and ~10^{12} Jones at NIR. The performance parameters of our phototransistors greatly surpass that of currently silicon photodetectors[4-5] and other reported photodetectors based on layered materials.[14-20] These ultrahigh performances of our multilayer InSe nanosheets

Journal of Materials Chemistry C Accepted Manuscript

 This journal is © The Royal Society of Chemistry 2012

phototransistors are mainly owing to high carrier mobility, narrow bandgap and direct band structures of InSe nanosheets. Such high performances make multilayer InSe nanosheets phototransistors very attractive for various applications in touch sensors panels, image sensors and solar cells.

Acknowledgements

This work is supported by National Natural Science Foundation of China (NSFC, No.61172001, 21373068), the National key Basic Research Program of China (973 Program) under Grant No. 2013CB632900.

Notes and references

[a] Key Lab of Microsystem and Microstructure of Ministry of Education, Harbin Institute of Technology, No. 2 YiKuang Street, Harbin, 150080, China. E-mail: hupa@hit.edu.cn.
[b] State Key Laboratory of Super lattices and Microstructures, Institute of Semiconductors, Chinese Academy of Sciences, Beijing 100083, China.
[c] Condensed Matter Science and Technology Institute, Harbin Institute of Technology, Harbin 150080, China.
[d] Center for Nano phase Materials Sciences, Oak Ridge National Laboratory, One Bethel Valley Road, Oak Ridge, TN 37831
[e] School of Materials Science and Engineering, Harbin Institute of Technology, Harbin, 150080, China.
[f] State Key Laboratory of Urban Water Resource and Environment, Harbin Institute of Technology, Harbin, 150080, People's Republic of China.
Electronic Supplementary Information (ESI) available: [details of any supplementary information available should be included here]. See DOI: 10.1039/b000000x/

1. A. Rogalski, J. Antoszewski and L. Faraone, *J. Appl. Phys.*, 2009, **105**, 091101.
2. M. Ettenberg, *Adv. Imaging*, 2005, **20**, 29-32.
3. E. H. Sargent, *Adv. Mater.*, 2005, **17**, 515-522.
4. E. Monroy, F. Omnès and F. Calle, *Semicond. Sci. Technol,*. 2003, **8**, R33.
5. R.-H. Yuang, J.-I. Chyi, W. Lin and Y.-K. Tu, *Opt. Quant. Electron.*, 1996, **28**, 1327-1334.
6. X. Gong, M. Tong, Y. Xia, W. Cai, J. S. Moon, Y. Cao, G. Yu, C.–L. Shieh, B. Nilsson and A. J. Heeger, *Science*, 2009, **325**, 1665-1667.
7. G. Konstantatos, I. Howard, A. Fischer, S. Hoogland, J. Clifford, E. Klem, L. Levina and E. H. Sargent, *Nature*, 2006, **442**, 180-183.
8. Z. Yin, H. Li, H. Li, L. Jiang, Y. Shi, Y. Sun, G. Lu, Q. Zhang, X. Chen and H. Zhang, *ACS Nano*, 2012, *6*, 74-80.
9. Y. Zhang, Y. Zhang, Q. Ji, J. Ju, H. Yuan, J. Shi, T. Gao, D. Ma, M. Liu, Y. Chen, X. Song, H. Y. Hwang. Y. Cui and Z. Liu, *ACS Nano*, 2013, **7**, 8963-8971.
10. X. Huang, Z. Zeng and H. Zhang, *Chem. Soc. Rev.*, 2013, **42**, 1934-1946.
11. M. Chhowalla, H. S. Shin, G. Eda, L.-J. Li, K. P. Loh and H. Zhang, *Nat. Chem.*, 2013, *5*, 263-275.
12. Z. Zeng, Z. Yin, X. Huang, H. Li, Q. He, G. Lu, F. Boey and H. Zhang, *Angew. Chem. Int. Ed.*, 2011, **50**, 11093-11097.
13. Q. He, Z. Zeng, Z. Yin, H. Li, S. Wu, X. Huang and H. Zhang, *Small*, 2012, **8**, 2994-2999.
14. P. A. Hu, Z. Wen, L. Wang, P. Tan and K. Xiao, *ACS Nano*, 2012, **6**, 5988-5994.
15. P. A. Hu, L. Wang, M. Yoon, J, Zhang, W. Feng, X. Wang, Z. Wen, J. C. Idrobo, Y. Miyamoto, D. B. Geohegan and K. Xiao, *Nano Lett.*, 2013, **13**, 1649-1654.
16. S. Lei, L. Ge, S. Najmaei, A. George, R. Kappera, J. Lou, M. Chhowalla, H. Yamaguchi, G. Gupta, R. Vajtai, A. D. Mohite and P. M. Ajaya, *ACS Nano*, 2014, **8**, 1263–1272.
17. L. Sanchez, D. Lembke, M. Kayci, A. Radenovie and A. Kis, *Nat. Nanotech*., 2013, **8**, 497-501.
18. T. R. Srinivasa, Y.-Y. Lu, R. K. U, R. Sankar, C.-D. Liao, C.-H. Cheng, F. C. Chou and Y.-T. Chen, *Nano Lett.*, 2014, **14**, 2800-2806.
19. R. B. Jacobs-Gedrim, M. Shanmugam, N. Jain, C. A. Durcan, M. T. Murphy, T. M. Murray, R. J. Matyi, R. L. Moore and B. Yu, *ACS nano*, 2013, **8**, 514-521.
20. F. Liu, H. Shimotani, H. Shang, T. Kanagasekaran, V. Zlyómi, N. Drummond, V. I. FaI'ko and K. Tanigaki, *ACS Nano*, 2014, **8**, 752–760.
21. M. V. Andriyashik, M. Y. Sakhnovskii, V. B. Timofeev and A. S. Yakimova, *Phys. Status Solidi*, 1968, **28**, 277-285.
22. S. Gopal, C. Viswanathan, B. Karunagaran, S.K. Narayandass, D. Mangalaraj and J. Yi, *Cryst. Res. Technol.*, 2005, **40**, 557-567.
23. G. Micocci and A. Tepore, *Sol. Energ. Mater*., 1991, **22**, 215-222.
24. M. A. Kenawy, H. A. Zayed and A. M. A. El-Soud, *J. Mater. Sci.-Mater. Electron*., 1990, **1**, 115-117.
25. M. M. El-Nahass, A-B. A. Saleh, A. A. A. Darwish and M. H. Bahlol, *Opt. Commun.*, 2012, **285**, 1221-1224.
26. D. Yoon, H. Moon, Y.-W. Son, J. S. Choi, B. H. Park, Y. H. Cha, Y. D. Kim and H. Cheong, *Phys. Rev. B* 2009, **80**, 125422.
27. Casiraghi, A. Hartschuh, E. Lidorikis, H. Qian, H. Harutyunyan, T. Gokus, K. S. Novoselov and A. C. Ferrari, *Nano Lett.*, 2007, **7**, 2711-2717.
28. W. P. Han, Y. M. Shi, X. L. Li, S. Q. Luo, Y. Lu and P. H. Tan, *Acta Phys. Sin.*, 2013, **62**, 110702.
29. S.-L. Li, H. Miyazaki, H. Song, H. Kuramochi, S. Nakaharaia and K. Tsukagoshi, *ACS Nano*, 2012, **6**, 7281-7288.
30. N. Jung, A. C. Crowther, N. Kim, P. Kim and L. Brus, *ACS Nano*, 2010, **4**, 7005-7013.
31. Y. K. Koh, M.-H. Bae, D. G. Cahill, E. Pop, *ACS Nano*, 2011, **5**, 269-274.
32. Y. Y. Wang, Z. H. Ni, Z. X. Shen, H. M. Wang and Y. H. Wu, *Appl. Phys. Lett.*, 2008, **92**, 043121.
33. V. Grasso and P. Perillo, *Solid State Comm*., 1977, **21**, 323-325.
34. E. D. Palik, *Handbook of Optical Constants of Solids*, Academic Press, New York, 1985.

The table of contents entry

Thickness dependent photon adsorption and phototransistors of multilayer InSe nanosheets have been demonstrated. Phototransistors based on multilayer InSe with a direct bandgap

Journal of Materials Chemistry C Accepted Manuscript

show broad spectural response and ultrahigh photoresponsivity and detectiviy.

Title: Ultrahigh Photo-responsivity and Detectivity in multilayer InSe nanosheets Phototransistors with Broadband Response

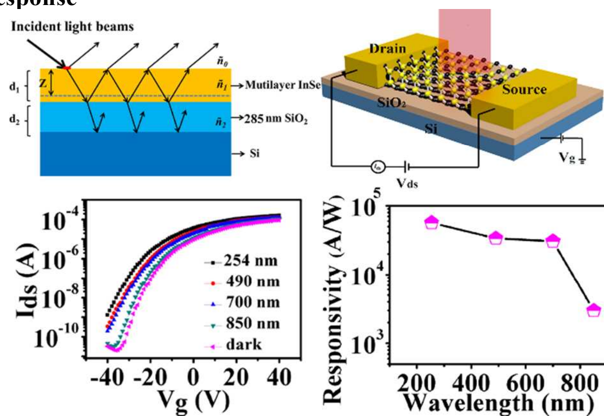

Journal of Materials Chemistry C Accepted Manuscript

 This journal is © The Royal Society of Chemistry 2012